ISSN: 3067-2384
Research Article
World Journal of Sensors Network Research

Radioassay of Lead Samples Using an Array of HPGe Detectors

Su-Yeon Park*, **Yeongduk Kim, & Jungho So**

Center for Underground Physics, Institute for Basic Science, Daejeon, 34126, Republic of Korea

***Corresponding author:** Su-yeon Park, Jungho So, Center for Underground Physics, Institute for Basic Science, Daejeon, 34126, Republic of Korea.

Submitted: 24 January 2025 **Accepted:** 27 January 2025 **Published:** 03 February 2025

https://doi.org/10.63620/MKWJSNR.2025.1015

Citation: *Park, S. Y., Kim, Y., & So, J. (2025). Radioassay of lead samples using an array of HPGe detectors. Wor Jour of Sens Net Res, 2(1), 01-05.*

Abstract

Lead is a common material for gamma-ray shielding but can contribute background signals in rare event searches, such as neutrinoless double beta decay. Single HPGe detectors cannot measure radioactivity below mBq/kg due to self-absorption and lead's high density. This study utilized a fourteen-channel HPGe detector array to measure contaminant activity in lead, accounting for screening effects.

Keywords: HPGe Detectors, Radioactivity Screening, Neutrinoless Double-Beta Decay, High Z-Number Materials, Lead Shielding, AMoRE-II Experiment, Screen Effect

Introduction

Materials with high atomic numbers (Z-numbers), such as lead and copper, are widely used for gamma-ray shielding in rare event search experiments [1]. However, as experiments scale up, the intrinsic radioactivity of these materials can contribute significant background signals, reducing detector sensitivity. The AMoRE-II experiment, targeting neutrinoless double beta decay of ^{100}Mo, uses lead shielding, necessitating stringent control of lead's radioactivity levels [2]. The requirement of ^{214}Bi activity is less than 300 μBq/kg.

This challenge is heightened for high Z-number materials due to screen effect and self-absorption, which hinder accurate radioactivity measurements [1, 3]. To overcome these obstacles, an array of fourteen HPGe detectors (array HPGe) has demonstrated improved efficiency for detecting ultra-low radioactivity compared to single HPGe detector systems [4-6]. This study introduces methods to account for the screen effect, enabling precise radioactivity assessments of ^{226}Ra and ^{228}Th decay chains in dense materials using the array HPGe.

Experiment

Six lead samples from four manufacturers were radio-assayed. Samples were processed into small pieces via waterjet cutting to minimize surface contamination. A 2-mm-thick layer was removed from each sample's surface, and the remaining material was cut into panels and blocks to fit between the array HPGe as shown in Fig. 1. The pieces were then washed with a nitric acid solution to eliminate residual contaminants like ^{214}Bi. Table 1 lists the type of lead sample, assay duration, mass, and radon level in the laboratory.

Table 1: Lead sample list and information for each lead sample dataset.

Manufacturer	Ingot / Brick	Time [day]	Mass [kg]	Radon activity [Bq/m^3]
Korea Zinc	Ingot	19	7.5	1.6 ± 0.5
Haekgwang #1	Brick	9	9.0	1.9 ± 0.5
Haekgwang #2	Brick	43	14.7	4.4 ± 1.0
Goslar	Brick	17	11.2	2.7 ± 0.5
Boliden #1	Brick	22	11.8	3.1 ± 0.7
Boliden #2	Brick	12	15.1	4.6 ± 1.8

The laboratory radon level was monitored using RAD7 under the operation of a radon reduction system (RRS) [7]. The RRS maintained a flow of boil-off nitrogen gas or radon-reduced air at 12 L/min to the copper shield enclosing the array HPGe. To assess intrinsic background contributions from radon and the detector system, seven background datasets (B1–B7) were collected with and without the RRS operation. Radon activity in the laboratory air and assay durations are provided in Table 2.

(a) (b)

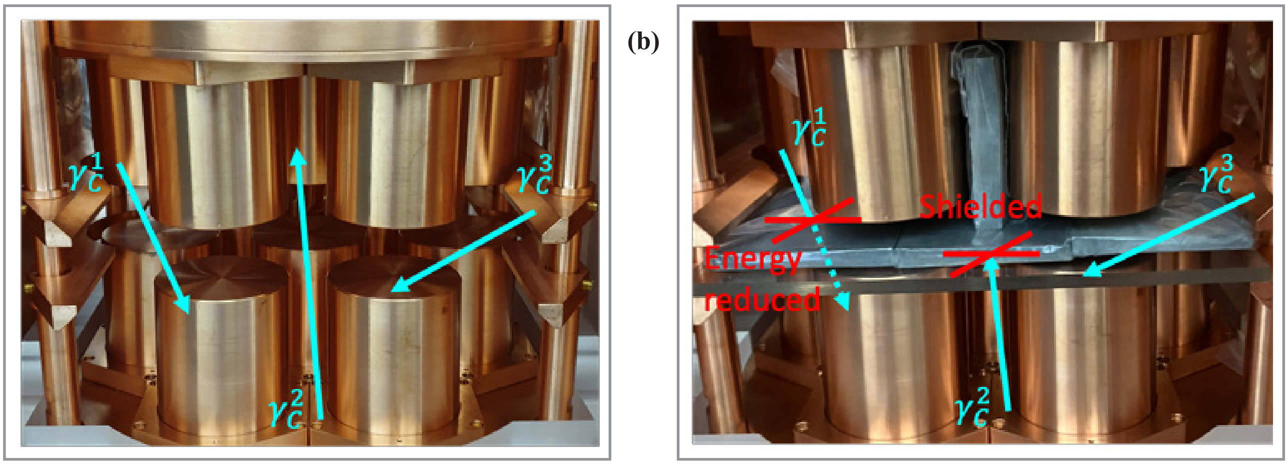

Figure 1: (a) The detected gamma-ray from the copper in the array HPGe. (b) Gamma-ray blocked by a lead sample.

Table 2: Background data list and information such as assay duration and radon level in the air in the laboratory.

	B1	B2	B3	B4	B5	B6	B7
Time [day]	59	33	37	58	93	69	26
Radon activity [Bq/m^3]	32 ± 4	4 ± 1	43 ± 8	1.7 ± 0.5	1.8 ± 0.6	0.9 ± 0.3	12 ± 4

Analysis

For ^{226}Ra decay chain analysis, background datasets collected with similar radon activity levels were matched to lead samples (e.g., Korea Zinc and Haekgwang #1 paired with B6, and other samples paired with B2). B6 was also used to analyze activities of ^{210}Pb and the ^{228}Th decay chain across all samples. The ^{210}Pb activity in the lead samples was determined by comparing their measured rates to that of Goslar lead, with a reference activity of 30 ± 1 Bq/kg [8]. ^{210}Pb activity was inferred by evaluating the rate in 100–220 keV bremsstrahlung region, which contributes 40% of the total rate in the 50–1162 keV energy range. Observed count rates from samples R_O and backgrounds R_B are listed in Table 3.

Table 3: Rates R_O and R_B observed from sample and background data sets, respectively, in units of /day.

Rate	Data set	^{208}Tl	^{214}Bi		^{210}Pb
		2615 keV	1120 keV	1765 keV	100-220 keV
R_o	Korea Zinc	2.44 ± 0.38	1.71 ± 0.30	1.70 ± 0.30	269620 ± 120
	Haekgwang #1	1.30 ± 0.39	1.94 ± 0.46	2.12 ± 0.48	184158 ± 140
	Haekgwang #2	2.54 ± 0.24	1.89 ± 0.21	2.33 ± 0.23	55437 ± 36
	Goslar	4.24 ± 0.53	2.81 ± 0.43	2.84 ± 0.43	8896 ± 24
	Boliden #1	4.36 ± 0.45	2.68 ± 0.35	3.05 ± 0.37	4019 ± 14
	Boliden #2	2.69 ± 0.50	2.96 ± 0.50	3.18 ± 0.52	3879 ± 18
R_B	B2	Not analyzed	1.33 ± 0.23	1.06 ± 0.18	Not analyzed
	B6	1.20 ± 0.13	0.92 ± 0.12	1.11 ± 0.13	558 ± 3

Due to bremsstrahlung interference, low-energy peaks (e.g., 583 and 609 keV) were not clearly visible in the spectrum. High-energy gamma-ray at 1120 and 1765 keV (^{214}Bi) and 2615 keV (^{208}Tl) were analyzed to determine the activity of the ^{226}Ra and ^{228}Th decay chains. Activities were assumed to be in equilibrium with ^{214}Bi and ^{208}Tl, respectively.

The rate of specific energy from a sample, R_S, is generally calculated as $R_S = R_0 - R_B$. However, for high Z-number materials like lead, the detection efficiency of gamma-ray from detector system depends on whether a sample is present due to the screen effect. Figure 1 shows an example of the detected gamma-ray emitted from the array HPGe, the blocked gamma-ray from observation, and the detected gamma-ray with energy loss. This effect can be incorporated into the formula as:

$$R_S = R_O - \frac{\epsilon_{wS}}{\epsilon_{woS}} R_B, \quad (1)$$

where ϵ_{wS} and ϵ_{woS} are the detection efficiencies with and without the sample, respectively [9]. The ratio $\frac{\epsilon_{wS}}{\epsilon_{woS}}$, term the screen effect factor α, can be determined using the GEANT4 simulation toolkit [10]. For background contributions, R_B is decomposed into components based on the source material.

Copper, which constitutes approximately 70% of the array HPGe (e.g., cryostats and. cold fingers), was assumed to be the dominant source of ^{208}Tl background signals. In this case, the corrected R_S is:

$$R_S = R_O - \alpha_C R_C, \quad (2)$$

where α_C represents screen effect factor of copper, and R_C represents the contribution from copper.

For ^{214}Bi, radon in the air and copper are the primary background contributors. The total background, R_B, is divided into two components: $R_B = R_C + R_A$, where R_A represents the radon contributions. With α_A, which represents screen effect factor of radon in the air, the corrected formula accounting for the screen effect is:

$$R_S = R_O - \alpha_C R_C - \alpha_A R_A, \quad (3)$$

Using background datasets B1 to B7, contributions to R_B from copper R_C and radon R_A were extracted for gamma-ray energies at 609, 1120, and 1765 keV. Linear fitting of R_B as function of radon levels provided the slope, representing R_A, and the y-intercept, representing R_C when radon levels are zero. Figure 2 shows R_B related to the radon level, extracted R_A and R_C. In conclusion, 39% and 11% of R_B in B2 and B6 were attributed to R_A, respectively.

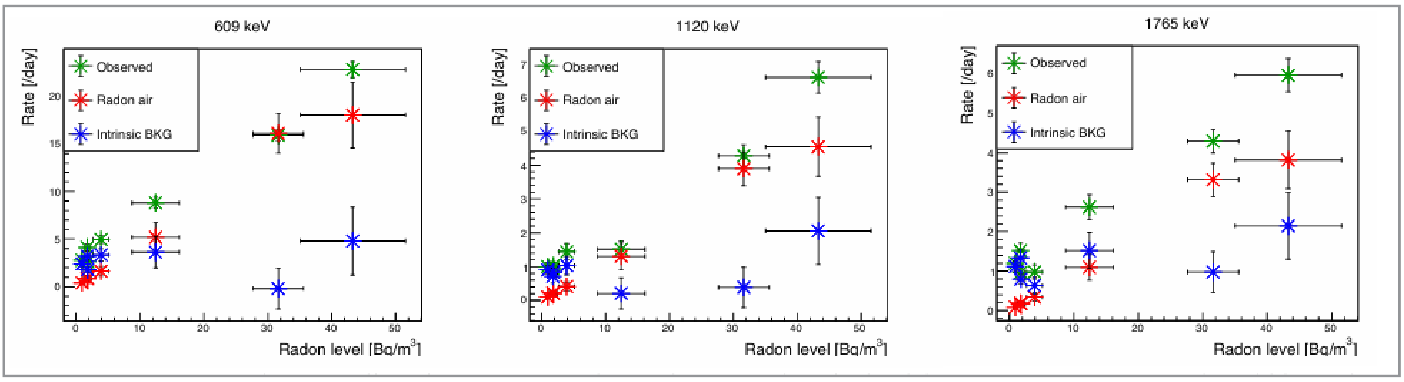

Figure 2: R_B, R_A, and R_C contributed 609, 1120, and 1765 keV energies obtained from B1 to B7. Green, red, and blue points represent R_B, R_A, and R_C, respectively.

To calculate α_C, the decays of isotopes in the copper components of the array HPGe were simulated with and without the six lead samples. Similarly, ^{214}Bi decay simulations were performed to determine α_A, accounting for radon in the air in the copper shield in the presence and absence of the lead samples. Additionally, the detection efficiency ϵ_S of gamma-ray emitted from the lead samples was simulated to account for self-absorption effects. The values of α and ϵ_S, obtained using the GEANT4 simulation toolkit, are provided in Table 4.

Table 4: Screen effect factors α_C and α_A were obtained from the GEANT4 simulation for 1120, 1765, and 2615 keV. Detection efficiency ϵ_S of gamma-ray emitted from the lead samples. The uncertainty is 16%.

Sample	α_C			α_A		ϵ_S (%)		
	^{208}Tl		^{214}Bi	^{214}Bi		^{208}Tl	^{214}Bi	
	2615 keV	1120 keV	1765 keV	1120 keV	1765 keV	2615 keV	1120 keV	1765 keV
Korea Zinc	0.96	0.85	0.98	0.89	0.85	1.75	2.69	2.72
Haekgwang #1	0.93	0.85	0.91	0.86	0.85	1.65	2.55	2.53
Haekgwang #2	0.92	0.81	0.91	0.78	0.76	1.51	2.21	2.21
Goslar	0.93	0.88	0.91	0.85	0.78	1.57	2.35	2.35
Boliden #1	0.90	0.76	0.97	0.85	0.78	1.68	2.52	2.55
Boliden #2	0.92	0.80	0.87	0.75	0.74	1.44	2.11	2.08

Result

The activities of ^{208}Tl, ^{214}Bi, and ^{210}Pb in the lead samples are summarized in Table 5. For each of ^{208}Tl and ^{214}Bi, two activity results were compared, derived with and without consideration of the screen effect. Systematic uncertainties, including detection efficiency calibration 12% [11] and geometrical uncertainties in simulations 10%, were estimated at 16%.

Table 5: Activities with or without the screen effect consideration for ^{214}Bi in units of μBq/kg. Four analysis results of the ^{208}Tl activity in units of μBq/kg obtained with or without considering screen effect. The activities of ^{210}Pb in units of Bq/kg searched.

Sample	^{208}Tl [μBq/kg]		^{214}Bi [μBq/kg]		^{210}Pb [Bq/kg]
	Without	With	Without	With	
Korea Zinc	< 484	< 528	285 ± 87 ± 45	319 ± 86 ± 50	963 ± 85
Haekgwang #1	< 169	< 187	< 555	388 ± 114 ± 61	661 ± 60
Haekgwang #2	197 ± 41 ± 31	211 ± 40 ± 33	< 307	248 ± 53 ± 39	196 ± 18
Goslar	560 ± 100 ± 87	575 ± 100 ± 90	508 ± 128 ± 79	551 ± 99 ± 86	30 ± 1 [8]
Boliden #1	517 ± 76 ± 81	536 ± 76 ± 84	416 ± 83 ± 65	467 ± 78 ± 73	12 ± 2
Boliden #2	< 342	< 370	426 ± 107 ± 67	490 ± 99 ± 77	12 ± 2

Given that Boliden #1 and #2 samples were from the same batch, their activities for ^{214}Bi and ^{208}Tl were weighted-averaged, yielding final values of 476 ± 61 ± 74 μBq/kg and 445 ± 51 ± 70 μBq/kg, respectively. Based on the results, Haekgwang #2 and Boliden were chosen for the AMoRE-II shields: a 20-cm-thick outer layer using Haekgwang #2 and a 5-cm-thick inner layer using Boliden. "This configuration will be used in the first stage of AMoRE-II with 90 Li_2MoO_4 scintillating crystals". Efforts are ongoing to identify low-radioactivity lead to meet the requirements for the final 5-cm inner shield.

The ^{210}Pb activity in the Boliden samples was approximately 12 ± 2 Bq/kg. This is attributed to the 22.2-year half-life of ^{210}Pb and the fact that the Boliden samples were procured approximately 20 years ago. It can be inferred that Boliden lead initially had a ^{210}Pb activity comparable to that of Goslar lead.

The activities in the lead samples were observed at sub-mBq/kg levels, measured over a few weeks for each sample. One key objective of this study was to evaluate the impact of applying the screen effect when measuring activity in high Z-number materials. Considering the screen effect increased the measured ^{208}Tl and ^{214}Bi activity by up to 11% and 15%, respectively.

Conclusion

This study evaluated the radioactivity levels of various lead samples using a fourteen-channel HPGe detector array, focusing on materials utilized in rare event experiments, such as neutrinoless double-beta decay searches. Key findings include the identification of ultra-low radioactivity in lead samples and the significant impact of the screen effect on detection accuracy. The analysis demonstrated that accounting for the screen effect increased measured activities of ^{208}Tl and ^{214}Bi by up to 11% and 15%, respectively. Based on the results, specific lead samples (Haekgwang #2 and Boliden) were selected for shielding in the AMoRE-II experiment. The study also highlighted the importance of simulations to account for the self-absorption effects in high Z-number materials. These insights are critical for enhancing sensitivity in rare event search experiments by minimizing background signals.

Acknowledgments

This work was supported by the Institute for Basic Science (IBS) funded by the Ministry of Science and ICT, Korea (Grant No: IBS-R016-D1).

References

1. Alessandrello, A., Cattadori, C., Fiorentini, G., Fiorini, E., Gervasio, G., Heusser, G., …. & Zanotti, L. (1991). Measurements on radioactivity of ancient Roman lead to be used as shield in searches for rare events. Nuclear Instruments and Methods in Physics Research Section B: Beam Interactions with Materials and Atoms, 61(1), 106-117.
2. Lee, M. H. (2020). AMoRE: A search for neutrinoless double-beta decay of 100Mo using low-temperature molybdenum-containing crystal detectors. Journal of instrumentation, 15(08), C08010.
3. Danevich, F. A., Kim, S. K., Kim, H. J., Kim, Y. D., Kobychev, V. V., Kostezh, A. B., …... & Voronov, S. A. (2009). Ancient Greek lead findings in Ukraine. Nuclear Instruments and Methods in Physics Research Section A: Accelerators, Spectrometers, Detectors and Associated Equipment, 603(3), 328-332.
4. Kim, G. W., Park, S. Y., Hahn, I. S. (2019). Simulation study for the half-life measurement of ^{180m}Ta using HPGe detectors. Journal of the Korean Physical Society, 75(1), 32-39.
5. Park, S. Y., Hahn, K. I., Kang, W. G., Kazalov, V., Kim, G. W., …... & Sala, E. (2021). Measurement of the background activities of a ^{100}Mo-enriched powder sample for an AMoRE crystal material by using fourteen high-purity germanium detectors. Nuclear Instruments and Methods in Physics Research Section A: Accelerators, Spectrometers, Detectors and Associated Equipment, 992, 165020.
6. Leonard, D. S., Hahn, K. I., Kang, W. G., Kazalov, V., Kim, G. W., Kim, …… & Sala, E. (2021). Development of an array of fourteen HPGe detectors having 70% relative efficiency each. Nuclear Instruments and Methods in Physics Research Section A: Accelerators, Spectrometers, Detectors and Associated Equipment, 989, 164954.

7. Ha, C., Jeong, Y., Kang, W. G., Kim, J., Kim, K. W., Kim, S. K., …… & Seo, K. M. (2022). Radon concentration variations at the Yangyang underground laboratory. Frontiers in Physics, 10, 1030024.
8. Ha, C., Adhikari, G., Adhikari, P., Jeon, E. J., Kang, W. G., Kim, B. H., …... & Yoon, Y. S. (2019). Initial performance of the high sensitivity alpha particle detector at the Yangyang underground laboratory. Nuclear Instruments and Methods in Physics Research Section A: Accelerators, Spectrometers, Detectors and Associated Equipment, 913, 15-19.
9. Thiesse, M., Scovell, P., Thompson, L. (2022). Background shielding by dense samples in low-level gamma spectrometry. Applied Radiation and Isotopes, 188, 110384.
10. Agostinelli, S., Allison, J., Amako, K., Apostolakis, J., Araujo, H., Arce, P., …… & Zschiesche, D. (2003). Geant4—a simulation toolkit. Nuclear Instruments and Methods in Physics Research Section A: Accelerators, Spectrometers, Detectors and Associated Equipment, 506(3), 250-303.
11. Park, S. Y., Hahn, K. I., Kang, W. G., Kazalov, V., Kim, G. W., ……. & Yoon, S. C. (2023). Detection efficiency calibration for an array of fourteen HPGe detectors. Applied Radiation and Isotopes, 193, 110654.